

Optical Interactions in the Junction of a Scanning Tunneling Microscope

Y. Kuk, R. S. Becker, P. J. Silverman, and G. P. Kochanski

AT&T Bell Laboratories, Murray Hill, New Jersey 07974-2070

(Received 12 March 1990)

Surface bias voltages induced on a scanning-tunneling-microscope junction illuminated with laser radiation are spatially measured for both metal and semiconductor samples. A surface photovoltage of ~ 0.3 V is observed for Si(111)-(7 \times 7), with large reductions in the vicinity of surface (subsurface) defects having midgap states. These reductions, attributed to a change in the recombination rate, have a typical surface screening distance of 15–25 Å. A small, atomically varying signal of 3–5 mV is observed on both metal and semiconductor samples and demonstrated to arise not from variation in photovoltage but from spatial variations in rectification efficiency.

PACS numbers: 61.16.Di, 72.40.+w, 73.25.+i, 73.30.+y

The interaction of radiation with matter is a subject that has occupied scientists for over a century. Early work using a variety of techniques concerned itself with effects measured on scales ranging from a few microns up to macroscopic distances,^{1–5} with the spatial resolution naturally depending on the probing technique. With the advent of the scanning tunneling microscope (STM), the possibility of studying elementary excitations on a scale of nanometers has been introduced. Since the STM is a nonlinear electronic device, these excitations manifest themselves as induced bias across the tunnel junction. Several optical mechanisms that may influence the tunneling bias come immediately to mind. First, thermoelectric emf's⁶ of a few millivolts can arise from differential heating of the tunnel junction by the absorbed radiation. Second, the whisker antenna geometry formed by the STM tip and sample produce an optical ac field across the junction, which gives rise to a small dc bias through rectification by the junction I - V characteristic.^{7,8} Third, if one of the junction electrodes is replaced by an appropriate semiconductor, photovoltage may result from the extra carriers created by absorption of incident radiation at or above the semiconductor band gap.

In recent experiments of Hamers and Markert,⁹ a visible-light laser was used to illuminate an STM junction consisting of a metal tip and Si(111)-(7 \times 7) sample. These workers reported an atomically varying photovoltage of 10–40 mV. The atomic variation was attributed to dynamic charging of surface states by extra carriers, with the various sites (dangling-bond sites in the faulted and unfaulted 7 \times 7 cell halves) undergoing different charging. This atomic-scale variation in photovoltage directly contradicts band-structure concepts in which variations in the induced bias should have a characteristic screening length extending over many sites. Further, the Coulomb interaction between surface sites due to this dynamic charging would be considerable.¹⁰ Taken together, these argue against an atomic variation in the charging of the various dangling-bond sites. It was also reported that the absorption of molecular oxygen created recombination centers on Si(111)-(7 \times 7) with a large reduction in induced bias near these centers,⁹ despite the

fact that oxygen adsorption on Si(111) has been shown to reduce the midgap state density responsible for efficient recombination.¹¹

In this Letter we report a series of experiments on a tunnel junction consisting of a metal tip and a metal or semiconductor sample, illuminated with laser radiation at or above the semiconductor indirect band gap. The resulting induced bias was measured spatially as both light-induced excess current and voltage. Most of the induced voltage (~ 300 mV) for the Si(111)-(7 \times 7) is found to be due to photovoltage, with large reductions occurring in the neighborhood (15–25 Å) of surface (subsurface) defects which increase the recombination rate due to the presence of additional midgap state density. A small variation (< 5 mV) on an atomic scale is seen on both metal and semiconductor samples. We suggest that this atomic signal is not due to dynamic charging by the extra carriers but rather to rectification by the spatially varying junction characteristic and/or small systematic errors inherent in the measuring process.

The experiments were performed in UHV (ultrahigh vacuum) conditions, using STM's that have been described elsewhere.¹² The optical field was produced with external HeCd, HeNe, and Nd-doped yttrium-aluminum-garnet lasers at incident powers of 2–20 mW, and photon energies of 2.94, 1.96, 1.17, and 0.95 eV. The STM's were modified by incorporating a small lens to focus the incident laser beam to a near-diffraction-limited spot, giving power densities up to 5000 W/cm² on the junction. The Si(111) [p type (boron, 0.7 Ω cm) and n type (arsenic, 0.7–5.0 Ω cm)] and Au(110) samples were cleaned *in situ* using conventional techniques, producing clean, well-ordered surfaces as determined with the STM. Further experiments were carried out on Si(001)-(2 \times 1) surfaces which showed a smaller photovoltage (~ 0.1 V), and cleaved InP(110)-(1 \times 1) surfaces which showed no optically induced voltage. These measurements along with the wavelength dependence, polarization dependence, and incident-angle dependence of the present samples will be reported in an extended paper.¹³

Figures 1(a) and 1(b) are spatially averaged junction

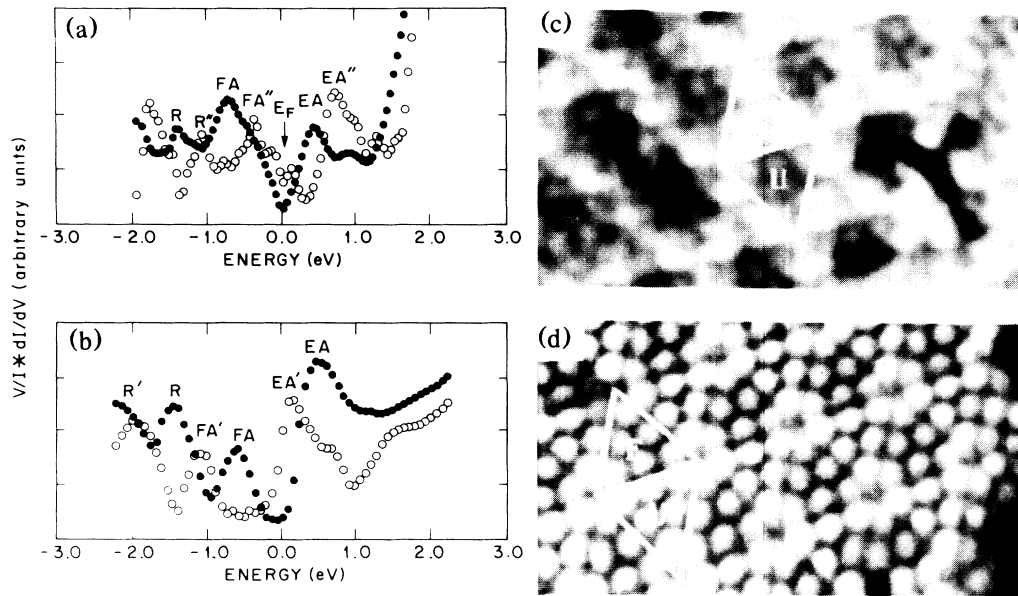


FIG. 1. Normalized conductance, which is proportional to electronic density of states for both (a) *p*- and (b) *n*-type Si(111)-(7×7). The corresponding photocurrent images of 120×70-Å area [(c), *p* type; (d), *n* type].

I-V characteristics which show the shift in the surface-state density,^{14,15} for both *n*- and *p*-type Si(111)-(7×7), that occurs under laser illumination above the semiconductor indirect gap. In both cases we see an essentially uniform displacement of the dangling-bond states across the spectrum, $\sim +0.3$ V for *p* type and ~ -0.35 V for *n* type with respect to the nonilluminated spectrum. This uniform shift demonstrates that the induced photovoltage is nearly the same at both adatom and rest-atom sites. Similar measurements performed on Si(111) using 0.95-eV radiation showed no induced bias. Figures 1(c) and 1(d) show photocurrent images for both *p*- and *n*-type materials. The photocurrent, current through the tunneling gap due to light-induced bias, was measured with zero external gap voltage as the tunneling gap is stabilized using an interrupted feedback loop. The spatial patterns exhibited by the *p* and *n* samples are quite different, with the corner adatoms of the faulted mesh half prominent in the *p*-type material, while the six adatoms in the unfaulted mesh half are prominent in the *n*-type material, but all twelve adatoms in a unit mesh are easily discerned. These images bear striking resemblance to the photovoltage images taken with a different interrupted feedback circuit in Ref. 9. The tunneling spectra in Figs. 1(a) and 1(b) immediately suggest the source of the spatial contrast in the current images: The photovoltage has set the quasi-Fermi level close to the highest-lying occupied adatom states for the *p*-type material, and close to the lowest-lying unoccupied adatom states for the *n*-type material. The highest occupied adatoms are the corner adatoms in the faulted half of the (7×7) unit mesh, while the lowest-lying unoccupied states occur in the unfaulted half of the unit mesh. For

both the *I-V* characteristics and the current images it is exactly as if a small "battery" had been placed in series with the tunnel junction, with no apparent atomic variation in the photovoltage. This is essentially the same as the CITS (current imaging tunneling spectroscopy) method originally used to image surface-state density on the (7×7) structure.¹⁴

How can one determine whether a spatial variation on the atomic scale exists? To address this, we have measured photovoltage shifts using spatially resolved tunneling spectroscopy.¹⁵ Moreover, we have varied the light intensity to investigate whether different surface states are filled (emptied) at different rates. Figure 2 shows a plot of induced voltage shift versus laser power density for both corner adatoms and rest atoms. Within the experimental errors (20 mV), there is no difference in photovoltage between these positions in the (7×7) unit mesh. Induced voltages at both sites initially increase linearly and asymptotically approach a saturation voltage of ~ 0.3 V. While this method is accurate, it is limited in sensitivity, leaving the possibility of atomic variations of small amplitude.

Rather than record spatial variations in photocurrent, which merely reflect the spatial localization of the dangling-bond electron states near the quasi-Fermi level, it is feasible to measure the effective induced bias directly by employing another interrupted feedback amplifier, similar to that which stabilizes the STM tip itself, in the circuit controlling the tip bias in a manner analogous to that in Ref. 9. This secondary feedback bias is the effective induced voltage, but opposite in sign. For this secondary loop, it is important to use *integrating* feedback with appropriate time constant and gain; *propor-*

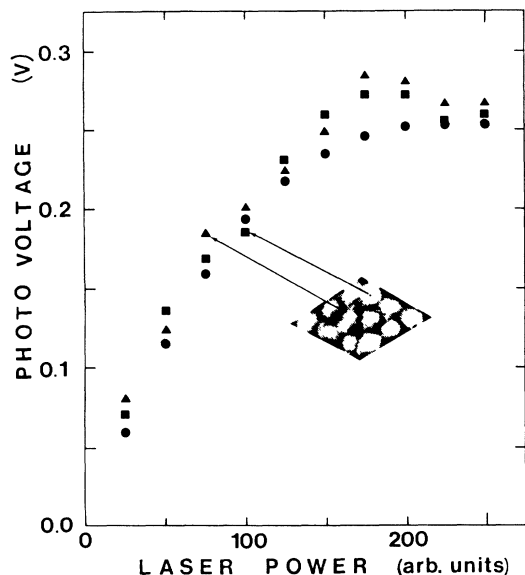


FIG. 2. Measured photovoltage as a function of laser power density. The circles indicate the average shift over (7×7) unit cell, the squares on corner adatoms, and the triangles on rest atoms.

tional feedback will always have an error dependent on the tunnel junction impedance and therefore on the set point of the primary feedback loop. The error signal for the proportional feedback may be a few tens of percent of the demanded voltage, giving an apparent photovoltage image containing residual traces of the electronic state density of the (7×7) dangling bonds. Figure 3 shows a tunneling image of *n*-type Si(111)- (7×7) and a simultaneously acquired induced-bias image. The darkest features represent an induced bias of near zero, while the brightest features are at ~ -0.25 V. A small signal (< 5 mV, but much less than that in Ref. 9) is yet present at atomic length scales and will be discussed below. The dark areas represent regions where the surface recombination rate is higher than in neighboring areas, lowering the induced voltage as determined by the rate equations.³ This is due to the presence of midgap states (most likely from trace metal impurities) arising from subsurface and surface defects, which have been shown to act as recombination centers in the bulk.¹¹ A cross section through the largest dark feature shows the spatial extent of the induced voltage reduction in this area. It is interesting to note that not all of the dark regions in the induced-bias image are matched by an obvious surface defect, while adatom vacancies in the (7×7) superstructure (possibly generated by H or O adsorption^{16,17}) do not have a large effect on the recombination rate. We have studied the effects of oxygen adsorption on the magnitude of the photovoltage, and find no change in photovoltage up to an exposure of ~ 4 L [1 L (langmuir) = 10^{-6} Torr sec], with an estimated coverage

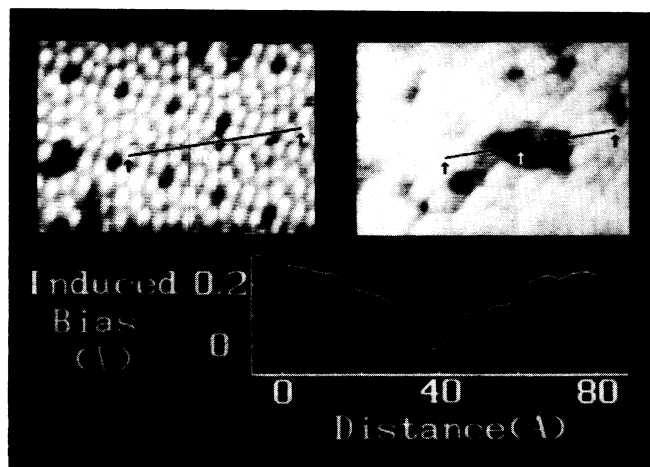


FIG. 3. An STM topograph of Si(111)- (7×7) and a simultaneously taken photovoltage image of 120×90 Å. The screening behavior is illustrated by the cross-sectional view of photovoltage along the solid line.

of 1 ML (ML denotes monolayer).¹³ At < 1 -ML coverage, oxygen absorption on the (7×7) structure evidently does not create additional midgap states to serve as recombination sites. The cross section in Fig. 3 through the large recombination center shows a surface screening length of 15 – 25 Å, compared to a bulk screening length of 500 – 600 Å as determined by the doping level. We suspect this short screening length is due to the high state density of adatom dangling bonds in the Si(111)- (7×7) superstructure and the extra carrier density due to optical absorption, in contrast to the identical screening lengths for bulk and surface for oxygen absorption on GaAs(110).¹⁸ The fact that we measure a saturation-induced voltage of ~ 0.3 V for both *n*- and *p*-type material indicates that the Si(111)- (7×7) adatom dangling bonds, which produce a large density of midgap states, themselves act as efficient recombination sites, limiting the maximum induced bias as demanded by the rate equations. A Demer potential, while decreasing the induced voltage for *p*-type material,⁹ would increase the bias for *n*-type material.

Several mechanisms have been considered to explain the small, atomic-scale induced voltage seen in Fig. 3. First, there may be residual feedback errors of a few mV since the amplifiers we use are not perfect integrators, and it is not practical to scan slowly enough to eliminate this source of error. We have used scanning speeds of 50 – 100 Å/sec while the gain is adjusted for critical damping. Second, thermoelectric emf's⁶ may arise in the junction due to heating of the tip and the sample by the optical radiation. While this temperature increase may easily account for a few mV of induced bias, we do not expect these emf's to vary much in spatial position. Finally, we consider the rectification of the optical field by the antenna configuration of the STM tip and sample.

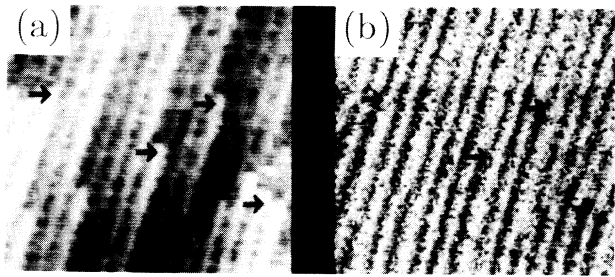


FIG. 4. An STM topograph of the Au(110)-(1 \times 2) (120 \times 120 Å) and a simultaneously taken light-induced current image.

The nonlinear I - V characteristic of the junction can vary on an atomic scale, due to changes in both state density and tunneling geometry. None of these mechanisms relies on a nonequilibrium carrier density. To explore this, we substituted an Au(110)-(1 \times 2) sample for the semiconductors in the tunnel junction. An image of this surface and the corresponding zero-bias photocurrent image is shown in Fig. 4. We clearly see a spatial variation in the photocurrent that corresponds exactly to the troughs in the Au(110) surface structure, even following the offsets as the microscope tip traverses steps. This current corresponds to an induced voltage of ~ 3 mV and varies on an atomic scale. We suspect this small signal is due to optical rectification caused by the changing junction geometry as the tip moves from filled row to missing row in the Au surface.

In summary, we find the dominant signal to be photovoltage which does not vary atomically, in contradiction to previously reported measurements on the Si(111)-(7 \times 7) surfaces. The recombination centers have a typical screening length of 15–25 Å, which is less than the bulk screening length of 500–600 Å for these samples. A small, atomic variation of < 5 mV is likely due to spatially varying rectification in the tunnel junction.

We acknowledge a helpful discussion with W. L. Brown, H. F. Hess, R. B. Robinson, and R. Wolkow.

¹*Proceedings of the Photoconductivity Conference, Atlantic City, New Jersey, 1954*, edited by R. G. Breckenridge *et al.* (Wiley, New York, 1956).

²W. L. Brown, W. H. Brattain, and C. G. B. Garrett, in *Semiconductor Surface Physics*, edited by R. H. Kingston (Univ. Pennsylvania Press, Philadelphia, PA, 1956), p. 111.

³R. A. Smith, *Semiconductors* (Cambridge Univ. Press, Cambridge, 1978).

⁴J. Clabes and M. Henzler, *Phys. Rev. B* **21**, 625 (1980).

⁵J. E. Demuth, W. J. Thompson, N. J. Dinardo, and R. Imbihl, *Phys. Rev. Lett.* **56**, 1408 (1986).

⁶J. M. Ziman, *Principle of Theory of Solid* (Cambridge Univ. Press, Cambridge, 1972), p. 235.

⁷T. E. Sullivan, P. H. Cutler, and A. A. Lucas, *Surf. Sci.* **62**, 455 (1977).

⁸A. Sanchez, C. F. Davis, K. C. Liu, and A. Javan, *J. Appl. Phys.* **49**, 5270 (1978)

⁹R. J. Hamers and K. Markert, *Phys. Rev. Lett.* **64**, 1051 (1990).

¹⁰An atomic-charge-superposition calculation shows that the total energy of the surface would increase by ~ 2 eV/(1 \times 1) through the Coulomb interaction in order to create an atomically varying bias of ~ 20 mV by dynamically charging dangling-bond sites. This energy is approximately that of the calculated energy differences between various Si(111) surface reconstructions.

¹¹N. J. Halas and J. Bokor, *Phys. Rev. Lett.* **62**, 1679 (1989).

¹²Y. Kuk and P. J. Silverman, *Rev. Sci. Instrum.* **60**, 165 (1989); R. S. Becker, B. S. Swartzentruber, J. S. Vickers, and T. Klitsner, *Phys. Rev. B* **39**, 10756 (1988).

¹³Y. Kuk, R. S. Becker, and P. J. Silverman (to be published).

¹⁴R. J. Hamers, R. M. Tromp, and J. E. Demuth, *Phys. Rev. Lett.* **56**, 1972 (1986).

¹⁵Ph. Avouris and R. Wolkow, *Phys. Rev. B* **39**, 5091 (1989).

¹⁶T. Sakurai, Y. Hasegawa, T. Hashizume, I. Kamiya, T. Ide, I. Sumita, H. W. Pickering, and S. Hyodo, *J. Vac. Sci. Technol. A* **8**, 259 (1990).

¹⁷F. M. Leibsle, A. Samsavar, and T.-C. Chiang, *Phys. Rev. B* **38**, 5780 (1988).

¹⁸J. A. Stroscio, R. M. Feenstra, and A. P. Fein, *Phys. Rev. Lett.* **58**, 1668 (1987).

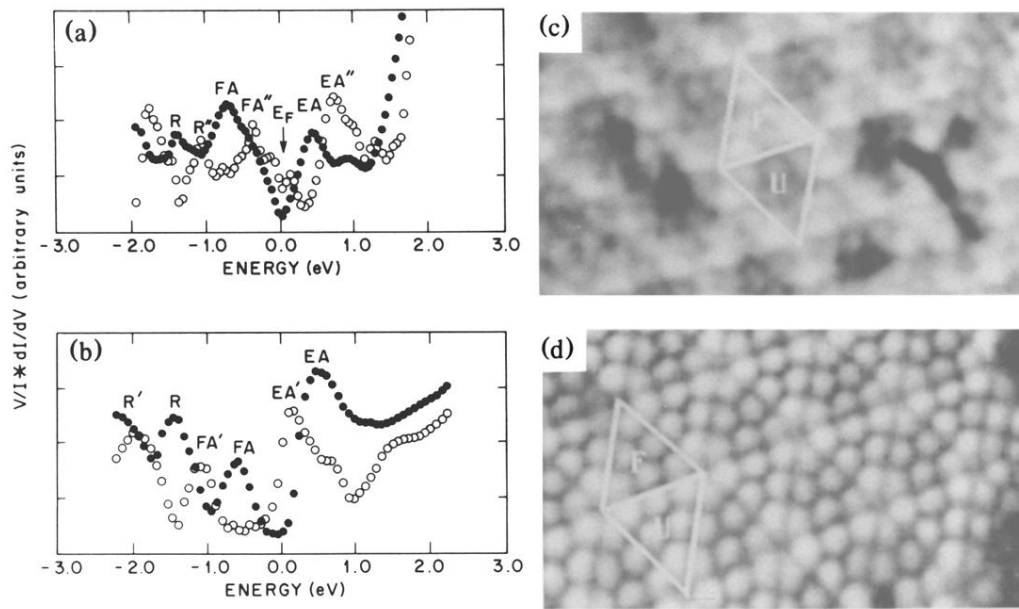


FIG. 1. Normalized conductance, which is proportional to electronic density of states for both (a) *p*- and (b) *n*-type Si(111)-(7x7). The corresponding photocurrent images of 120x70-Å area [(c), *p* type; (d), *n* type].

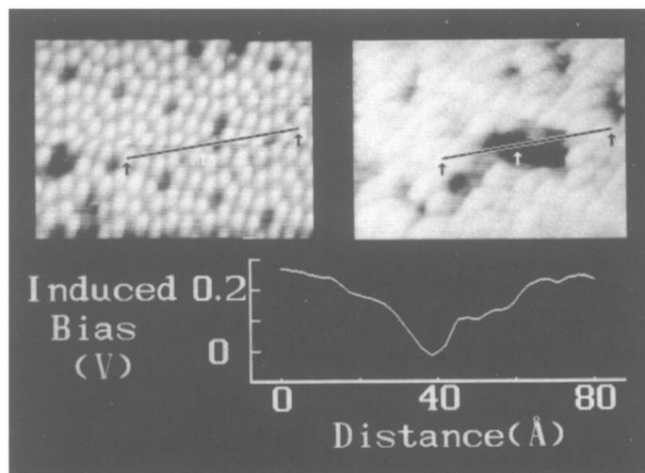


FIG. 3. An STM topograph of Si(111)-(7×7) and a simultaneously taken photovoltage image of 120×90 Å. The screening behavior is illustrated by the cross-sectional view of photovoltage along the solid line.

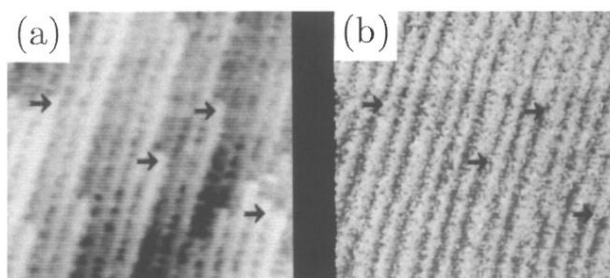


FIG. 4. An STM topograph of the Au(110)-(1×2) (120×120 Å) and a simultaneously taken light-induced current image.